

ALMA MATER STUDIORUM  
UNIVERSITA' DI BOLOGNA

SCHOOL OF ENGINEERING

-Forlì Campus-

SECOND CYCLE MASTER'S DEGREE in  
AEROSPACE ENGINEERING  
Class LM-20

GRADUATION THESIS IN:

Aerospace Structures

**Influence of consolidation pressure on interfacial  
properties of AM components**

**CANDIDATE:**

Chiara Pennuti

**SUPERVISORS:**

Dr. Enrico Troiani

Dr. Giacomo Struzziero

Dr. Alex Skordos

**EXAMINER:**

Dr. James Kratz

Academic Year 2021/2022



MASTER'S THESIS 2023

**Influence of consolidation pressure on interfacial  
properties of AM components**

Chiara Pennuti

In collaboration with:

Cranfield University  
*School of Aerospace, Transport and Manufacturing*  
Composites and Advanced Materials Centre

and

Empa, the Swiss Federal Laboratories for Materials Science and Technology  
*Laboratory of Mechanical System Engineering*  
Composites Group

EMPA  
Dübendorf, Switzerland 2023



---

*"Tiriamo avanti"*  
- Benito Pennuti (1924-2018)



---

## Abstract

This study extends the analysis of current research on partially cured components behaviour of Carbon Fibre Reinforced Polymers, with the aim of decreasing the amount of scrapped parts generated by an unsustainable manufacturing production, lowering the processing time, and allowing the creation of thicker and more complex shapes while reducing the risk of generating thermal gradients and residual stresses across the thickness of the component. It has been recently demonstrated that the mechanical interfacial properties are retained as long as the level of partial cure of the layers bonded is below the gelation point. This project aims at addressing how the adhesive fracture toughness is influenced by both degree of cure and consolidation pressure. This is investigated through mode I delamination tests and concurrently, thermo-mechanical simulations are developed to validate both the curing cycles chosen for the manufacturing of the specimens and the peel-off analysis. The outcomes of the project point out that an increase in consolidation pressure for the configuration where one uncured layer is bonded with a partially cured one at 20% of degree of cure can have beneficial effects on the mechanical properties of the material.

Keywords: Additive Manufacturing, Layer by Layer Curing, Continuous Fibres, Interfacial Properties, Consolidation Pressure, Finite Elements Analysis.





---

## Acknowledgements

I would like to give my warmest thanks to my supervisors, Dr. Enrico Troiani, for encouraging hands-on experiences and giving me the opportunity to enhance my studies abroad, Dr. Giacomo Struzziero, for his guidance and advice that carried me through all the phases of this project, and Dr. Alex A. Skordors, for his invaluable mentorship and continuous support.

I would like to address a special thanks to Marcel Rees, who helped me during my laboratory work. My gratitude extends to all my friends, colleagues, and lab mates at Empa, for a cherished time spent together in the labs and outdoors around Zurich. My appreciation also goes out to my family for the encouragement and support showed all through my studies.

Lastly, I am extremely grateful to the doctors, the nurses, and the healthcare workers at IRST "Dino Amadori" and AUSL Romagna for their hard work, constant care, and compassion. Thank you all for giving me hope and a reason to smile during my troubled times.



---

# Contents

<b>List of Figures</b>	<b>xiii</b>
<b>List of Tables</b>	<b>xv</b>
<b>1 Introduction</b>	<b>1</b>
1.1 Background . . . . .	1
1.2 Aim and objectives . . . . .	4
1.3 Thesis outline . . . . .	4
<b>2 Literature Review</b>	<b>7</b>
2.1 Cure-induced defects in composite manufacturing . . . . .	7
2.2 Joints and joining techniques . . . . .	9
<b>3 Materials and Methodology</b>	<b>13</b>
3.1 Pre-preg material . . . . .	13
3.2 Cure kinetics characterisation . . . . .	13
3.3 Manufacturing process . . . . .	15
3.4 Experimental set up . . . . .	18
3.5 Finite Element model . . . . .	19
3.5.1 Cure kinetics validation . . . . .	19
3.5.2 Peel-off tests . . . . .	22
<b>4 Results and Discussion</b>	<b>25</b>
4.1 Cure kinetics . . . . .	25
4.2 Peel-off tests . . . . .	27
4.3 Finite Element model . . . . .	32
4.3.1 Cure kinetics validation . . . . .	32
4.3.2 Peel-off tests . . . . .	34
<b>5 Conclusions and Future Work</b>	<b>37</b>
5.1 Conclusions . . . . .	37

5.2 Future work . . . . .	38
<b>Bibliography</b>	<b>41</b>

---

# List of Figures

1.1	Airbus A350 XWB structure composition. Image reprinted from [1] and available via license Creative Commons Attribution 4.0 International . . . . .	1
3.1	Standard and Modulated analysis equipment . . . . .	14
3.2	Manufacturing of the laminate . . . . .	17
3.3	Equipment used during the manufacturing process . . . . .	17
3.4	Specimens obtained from the laminate manufactured . . . . .	18
3.5	Zwick Z010 machine set-up for the peel-off tests . . . . .	18
3.6	Schematic model of the dimensions of the component . . . . .	20
3.7	Mesh of the 0/0 configuration, focus on the thickness of the laminate . . . . .	20
3.8	Temperature profile applied to cure the 0/0 configuration . . . . .	21
3.9	Schematic model of the part designed on Marc © . . . . .	22
3.10	Boundary conditions applied on two nodes of the upper layer of the model . . . . .	24
4.1	Characterisation of the cure kinetics . . . . .	26
4.2	DiBenedetto curve . . . . .	27
4.3	Configurations with two layers below gelation (1 bar consolidation pressure) . . . . .	28
4.4	Configurations with one layer above gelation (1 bar consolidation pressure) . . . . .	28
4.5	Comparison between average $G_A$ for configurations at 1 bar and 2 bar of consolidation pressure . . . . .	30
4.6	Comparison between average $G_A$ for the 0/20 configuration at different consolidation pressures . . . . .	31
4.7	0/20 configuration at 10 bar of consolidation pressure . . . . .	32
4.8	Validation of the cure kinetics . . . . .	33
4.9	Comparison between the model of the cure kinetics and the FE model . . . . .	34

4.10 FE simulation for $G_A$ equal to 306.09 N/m and focus on the upper nodes simulating the contact with the peel-off machine; the reaction force in the colourmap is in N . . . . .	34
4.11 Reaction Force Z on the nodes of the FE model for $G_A$ equal to 306.09 N/m . . . . .	35
4.12 Reaction Force Z on the nodes of the FE model for $G_A$ equal to 21.43 N/m . . . . .	36

---

# List of Tables

3.1	Configurations chosen for the development of the project . . . . .	15
3.2	Thermal profiles for different degrees of cure . . . . .	16
3.3	Properties of the material . . . . .	21
3.4	Properties of the materials . . . . .	23
4.1	Cure kinetics fitting parameters . . . . .	25
4.2	DiBenedetto parameters . . . . .	27
4.3	Average $G_A$ and relative standard deviation for configurations at 1 bar of consolidation pressure . . . . .	29
4.4	Average $G_A$ and relative standard deviation for configurations at 2 bar of consolidation pressure . . . . .	29
4.5	$F_z$ : comparison between delamination tests and FE simulations . . .	35





---

# 1

## Introduction

### 1.1 Background

Nowadays, the use of composite materials experienced a boost in the manufacturing of complex shapes and structures in several fields, going from aerospace, to automotive, to renewable energy, and to nuclear engineering. An example of their usage is the incorporation of more than 50% carbon fibre composites in aircraft models such as the Boeing 787 Dreamliner and the Airbus A350 XWB, where fuselage, wings, stabilizers and turbine housings are manufactured primarily from polymeric composites [1, 2]. This is mainly due to the high-performance characteristics of these materials, which can guarantee high mechanical strength and high fatigue and corrosion resistance while maintaining a low weight. The latter may be the most important characteristic for some of the aforementioned industries as the aerospace one. Indeed, a reduction in weight leads to lower fuel consumption and CO<sub>2</sub> emission.

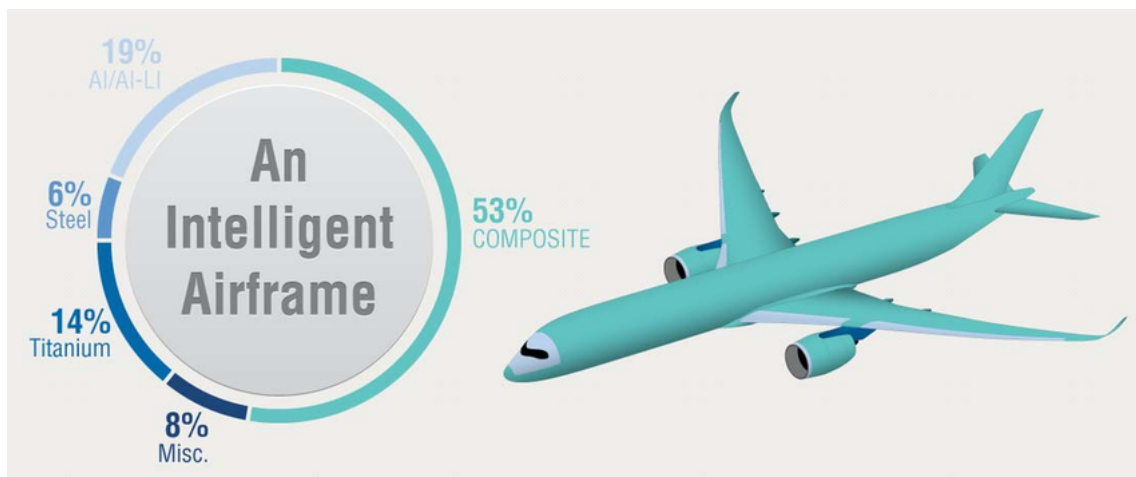


**Figure 1.1:** Airbus A350 XWB structure composition. Image reprinted from [1] and available via license Creative Commons Attribution 4.0 International

The greatest challenge that humanity and our planet are currently facing is climate

change, and the use of composite materials has already contributed to the reduction of greenhouse gas emissions. Nevertheless, it must be underlined that the extraction of carbon, the production of the composites, and their recycling are not green and sustainable processes. This implies that it is crucial to develop and improve the manufacturing process in order to waste as little material as possible, to minimise the energy consumption of the process itself [3], and to explore composite recycling strategies to efficiently separate the resin systems from the reinforcing fibres, avoiding the quality degradation of the latter [4].

At the moment, the market is demanding ever higher number of composite parts for different applications, raising the carbon fibre demand from 35400 tonnes in 2008, to 70800 tonnes in 2014, reaching up to 120000 tonnes in 2019 [4]. To cope with this increasing demand, the industry is expected to develop more efficient and quicker manufacturing methods. For instance, when it comes to the curing process, it is possible to speed up this sub-phase of the production by increasing the temperature of the cure cycle. However, due to the strong non-linearity of the physics governing cure processes, when undergoing high temperature cure cycles thermosetting resins are extremely sensitive to temperature overshoots. The latter may be a source of defects, low performance, or failure of the material. Indeed, aggressive cure cycles could generate thermal gradients through the thickness of the component hence, the formation of defects and residual stresses, leading to a decrease of mechanical properties of the material [5]. In thick components this exothermic behaviour could also lead to undesired degradation of the resin system, making the manufactured part prone to failures and hence, unusable. Therefore, the industry tends to rely on conservative and generic cure profiles, which favour low probability of exothermic failure, but increase the duration of the process and the manufacture cost [6].

Furthermore, when it comes to manufacturing, companies implement trial-and-error approaches, and experience-based designs are preferred to Finite Element (FE) simulations. Time and effort is spent to gain a deep understanding of the process to be used for a specific material and for the manufacturing of a specific component; hence, companies might be reluctant to venture towards new campaigns which cannot give certainty of better performance, and absence of risks in the manufacturing. Another downside of FE simulations is that the certification of the new process implemented could take years, often cancelling the benefits of creating such FE models. Nevertheless, the current production practice introduces difficulties in the creation of parts which are good and ready to be used at the first trial and limits the number

of components that can be manufactured, generating a gap between the industry production and the request of the market. Such unsustainable manufacture chain is characterised by a significant waste of material (e.g., scrapped parts) and energy consumption, which cannot be tolerated anymore in the race towards net zero emissions.

In the last decades, research on the optimisation of composite manufacturing was undertaken. Researchers have demonstrated that optimal cure profiles could minimise both process time and temperature overshoots by about 40% [5], achieving a reduction of energy consumption and avoiding thermal gradients through the thickness of the components. Moreover, Additive Manufacturing (AM) made its way to composites production, representing a viable alternative to Automated Fibre Placement (AFP), combining impregnation, deposition, and curing stage into a single one.

In recent years, Cranfield University and the University of Bristol (UK) put forward a new concept of manufacturing of advanced thermosetting composites, called Layer by Layer (LbL) curing [7], and paved the way to new research and investigation on the matter. This approach consists in curing a composite component layer by layer endorsed by the fact that interfacial properties are retained as long as the preceding layer has not cured above gelation at the time the new layer is laid upon. Such procedure would have the great advantage of curing only a fraction of laminate thickness at a time, allowing cure cycles to reach higher temperatures and shortening the whole processing time, while keeping comparable mechanical performances with components manufactured using standard processes.

The Layer by Layer method combined with useful tools as accurate cure kinetics and FE simulations could drastically optimise the manufacturing of composite materials. Nevertheless, further studies need to be carried out to assess the possible application of this manufacturing process for adhesive bondings and for bonding in joints by means of partial curing. Indeed, during the last decades, polymers and epoxy resins have been object of tremendous R&D activities to increase their adhesion properties, as composites are usually characterised by inherently poor adhesion properties due to their surface conditions [8, 9]. Studies focused on analysing the mechanical properties of the material showed that it is possible to find a level of partial cure which does not cause significant drops in the mechanical performances of the material [10, 11]. However, to fully take advantage of the new manufacturing concept, a through investigation into the science of partially cured components need to be undertaken.

A thorough research on the development of a truly additive process can simplify the production procedure from highly non-linear to linear, leading to less process-induced defects while achieving good interface properties. Adding to this the development of FE simulations, the final goal is the production of parts which are ready to be used after the first trial, in compliance with the standards to enter the market, and a decreased waste of scrapped material.

### 1.2 Aim and objectives

In this context, the project developed in this thesis aims at controlling the interfacial properties of consolidated and partially cured parts when undergoing different levels of consolidation pressures. This will be achieved by investigating and studying the bonding and the delamination processes of these parts. The objectives set up to drive the project are:

- Characterisation of the cure kinetics of the resin system present in the material;
- Manufacturing of specimens with different degree of cure and levels of consolidation pressure;
- Development of a mechanical and coupled thermo-mechanical FE model representative of the consolidation and delamination processes;
- Assessment of the interfacial properties through peel-off tests and mapping of the dependence of the former on the degree of partial cure of the bonded layers.

### 1.3 Thesis outline

Chapter 1 presents the background of the topic; the aim and objectives of the research developed in this thesis project, and defined the structure of this manuscript. Chapter 2 of this thesis presents a literature review, which aims at reviewing the state of the art on cure-induced defects minimisation in manufacturing of composite materials and joining techniques.

In Chapter 3, the material used in the project is presented and the methodology used to assess each part of the project are explained. In particular, Chapter 3 describes

the process of the characterisation of the material, from the specimen preparation to the analytical models, focusing on the manufacture and cure of the specimens, as well as the experimental tests and FE set up.

Chapter 4 shows and discusses the results obtained from the characterisation of the material, the experiments, and the FE models.

Chapter 5 summarises final considerations and the next points to investigate in future works are presented.



---

# 2

## Literature Review

This chapter aims at reviewing the state of the art on cure-induced defects minimisation in manufacturing of composite materials and joining techniques.

### 2.1 Cure-induced defects in composite manufacturing

As the composite sectors expands, thick and complex shaped laminates have found several applications and have become more and more common in aerospace, military, wind, marine and civil structures. A further increase in the usage of thick composites parts relies heavily on the successful manufacturing of parts with high quality at low cost. However, the low thermal conductivity of composites and the high heat of reaction generated during cross-linking polymerisation make the curing of thick parts a real challenge. One of the main causes of defects in composite manufacturing is indeed the thickness of the components, which can lead to large temperature overshoots at the midpoint of the laminate due to exothermic reaction and low thermal conductivity of the matrix [12–15]. As a consequence, the rise of significant thermal gradients and temperature peaks are known to generate residual stresses, polymer degradation, matrix cracking, and produce a non-homogeneous cure along the thickness direction [12, 16, 17]. Therefore, the manufacturing cure cycles need to be optimised to minimise thermal gradients throughout the part.

It is fundamental to acquire a deep and full knowledge of the initial stress state of a part in order to consider its in-service performances. Residual stresses can be problematic when it comes to the reliability of the part manufactured and a thorough design of a component cannot neglect this aspect since it is critical in terms of safety [18]. The presence of stresses can modify the mechanical properties of the laminates and thus, the in-service life of composite parts. This occurs by introducing matrix cracking and delamination, which are known to be a major pattern of

failures of composite materials. Furthermore, an initial stress state can also cause deformation (e.g. warpage) in the geometry of the component. This issue can be sometimes overcome during the designing phase of the part itself. Moreover, high temperature peaks are also known to be the cause of the aging and degradation of the matrix, which lead to mass loss, deterioration of properties, shrinkage, and cracking. The degradation of the matrix is a complex and coupled process where heat, moisture, and oxygen are transported into the material, which changes chemically, affecting its behaviour at the ply and laminate level. This can sometimes generate matrix cracking, which enhances oxygen infiltration, greater material changes, and more cracking, leading to a potentially unstable situation [19]. Lastly, thermosetting composites are highly sensitive to temperature, and thermal gradients across the thickness of a component can lead to a non-uniform distribution of degree of cure across the cross-section of the component, which introduces residual stresses [20].

All the aforementioned issues represent limiting factors in the application of Carbon Fibre Reinforced Polymers (CFRPs) to structures, due to its defects and the uncertainty of the behaviour of the mechanical properties of the material. Currently, the Manufacturer Recommended Cure Cycle (MRCC) is often an inadequate cure cycle for thick composites. Large out-of-plane temperature gradients and mid-plane heat generation are neglected, leading to the generation of the already mentioned flaws during the manufacturing of the part. Nevertheless, the reduction of processing temperature of thick composites should reduce thermally induced residual stresses [16], and thus, manufacturing defects [21]. However, this is likely to increase the curing time. Therefore, researchers proposed a passive solution to this problem, consisting in optimising and adjusting the cure cycle to decrease temperature overshoots, reducing the generation of defects while taking into account the thickness of the component. [3, 6, 15, 20, 22, 23]

During the past decades, researchers applied optimisation methodologies to the manufacturing process simulation, aiming at creating a first-time-right design and mitigating the generation of manufacturing defects [15, 20, 22]. Due to the complexity of the process and the interdependent nature of the different phenomena governing it, single objective optimisations were not meaningful and soon paved the way to multi-objective optimisations. Indeed, single objective optimisations would only focus on one characteristic of the process (e.g. optimal cure cycles to minimise cure time, residual stresses, or temperature overshoots) without taking into account that other objectives could worsen below acceptable levels. Therefore, researchers



developed a more realistic analysis by building fitness functions comprising two or more objectives, adding quality and cost related objectives for different manufacturing processes [23]. This led to the creation of methodologies for the optimisation of composite production, decreasing the manufacturing time and defects generation. However, these kind of optimisations were still not able to fully address the issue of the thickness of the part manufactured. Indeed, a weight was selected for every objective and thus, a limited exploration of the multidimensional objective space was achieved, incorporating constraints as in pure single objective optimisations [6]. Therefore, further studies [3,6] used multi-objective optimisation setting to address the cure profile selection problem, trying to minimise simultaneously both the cure duration and the temperature to find the optimal cure cycle for thick and ultra-thick components for wind and aerospace applications.

In recent years, in the wake of applying the concept of 3D printing to thermosetting composites, a new active solution to reduce process-generated defects in thick components has been put forward. This new manufacturing technique is called Layer by Layer (LbL) curing, and consists in an additive manufacturing process which allows to reduce temperature overshoots by curing components layer by layer. The concept of this new manufacturing route is indeed the one of curing the layers during the deposition, accelerating the consolidation process and reducing the curing time up to a 40% in thick laminates [7]. The feasibility of this process has been addressed in previous work [7] showing that the mechanical integrity of the products manufactured with this technique was acceptable. Further studies [10] measured and confirmed that the mechanical properties of the material when partially cured were retained. In particular, the aim of the latter work was to study the impact of the partial cure on the bonding between subsequent layers. The results of this work showed that a configuration where the layers were both characterised by a level of partial cure below the gelation point could allow the material to keep a good adhesive fracture toughness while reducing processing time and keeping a low thermal gradient along the thickness [10].

## 2.2 Joints and joining techniques

The increased use of composite materials in manufacturing of structures and for instance in primary aircraft structures such as wings, pressurised fuselage, and empennage, led to the need of optimising joining techniques to enable the manufacturing of highly integrated structures [24]. Currently, composite parts are produced

separately and then assembled together with other FRP or metallic parts using mechanical fasteners as bolts and rivets, adhesives, or combining the two technologies to create a hybrid bolted/bonded joint [11, 25]. Albeit necessary, joints represent the weakest link in the structures, constituting the site of potential damage initiation and failure, decreasing the robustness of the materials due to its heterogeneous character, and hence compromising the structural integrity of the component [26].

Mechanical fasteners are known to behave as stress concentrators and statistics show that approximately 70% of the failure of structures is initiated from joints [27]. This issue gets more severe when dealing with composite structures. These materials, indeed, are generally brittle, showing nearly linear characteristics before failure, and hence little local yielding and stress redistribution around fastener holes. Additionally, composites are anisotropic materials, which makes them susceptible to delamination and prone to high-stress concentration and low transverse strength of joints. Adhesive bondings might be considered the alternative method with the highest potential, as they can achieve full efficiency, particularly for simple joint configurations involving thin composite structures, while being continuous and lightweight. Nevertheless, they suffer drawbacks, such as the lack of efficient methods for inspecting the joints, surface preparation of the adherents prior to joining, and sensitivity to interlaminar delamination [11, 25]. Therefore, in aerospace applications adhesive bondings are usually replaced by hybrid joints. The latter mix together the advantages of bonding and mechanical fastening by not altering the structural properties of the composite while improving the static strength and fatigue resistance [28–30].

An alternative to the joining techniques previously introduced is the use of a co-curing process to join subcomponents together during the manufacturing. This is an efficient joining method where both the curing and the bonding processes for the composite structures can be achieved simultaneously [31]. Differently from a conventional adhesive method, it does not require surface treatment or additional adhesive joining processes. The bonding is accomplished by means of the excess resin extracted from composite materials during the consolidation. A variation of the co-curing process exploits the retained bonding properties of partially cured parts. This new manufacturing technique was studied as a bonding method in [11] as a tool to reduce complexity, time, and cost of the co-curing process. In particular, the latter work was focused on the manufacturing of specimens with different degrees of partial cure and on their performance in mode I delamination. The results showed that an uncured layers placed upon a partially cured ones could bond properly and

lead to good adhesive fracture toughness if kept below gelation. To gain a complete understanding of this manufacturing process and its applications, it is fundamental to study how the interfacial properties of the specimens are affected by the degree of cure, pressure, and temperature. In this manuscript, the work done by [10, 11] will be carried on and developed by investigating the interfacial properties varying the level of partial cure and the pressure applied during the finalisation of the curing process.



---

# 3

## Materials and Methodology

This chapter presents the materials chosen and the methods applied to investigate the influence of consolidation pressure on interfacial properties of consolidated parts. The characterisation of the cure kinetics is reported, followed by the manufacturing process and the experimental set-up. Lastly, two FE models are developed to validate both the cure kinetics and the delamination experiments.

### 3.1 Pre-preg material

The prepreg used in this project is a unidirectional (UD) carbon fiber preimpregnated with hot melt epoxy resin.

### 3.2 Cure kinetics characterisation

A chemical characterisation campaign of the material was performed running two isothermal (100°C, 120°C) and one dynamic (1°C/min) analysis through the use of a Differential Scanning Calorimetry (DSC). The machine available in the laboratory for such tests was the Netzsch DSC 204 F1 Phoenix and it can be seen in Figure 3.1.

In order to run standard and modulated DSC analysis, it was necessary to create the specimens to be tested in the machine. Around 6 mg of prepreg were cut from an uncured strip and placed in a pan. A lid was then clamped on the pan as showed in Figure 3.1 and the latter was positioned in the DSC machine for the test. In order to build the kinetics of the resin system inside the prepreg, a fitting procedure of the results coming out from the isothermal and dynamic tests was necessary. The fitting was performed through Microsoft Excel Solver and allowed the evaluation of the parameters to be used in the autocatalytic model with explicit diffusion which describes the relationship between reaction rate, degree of cure, and temperature as follows:

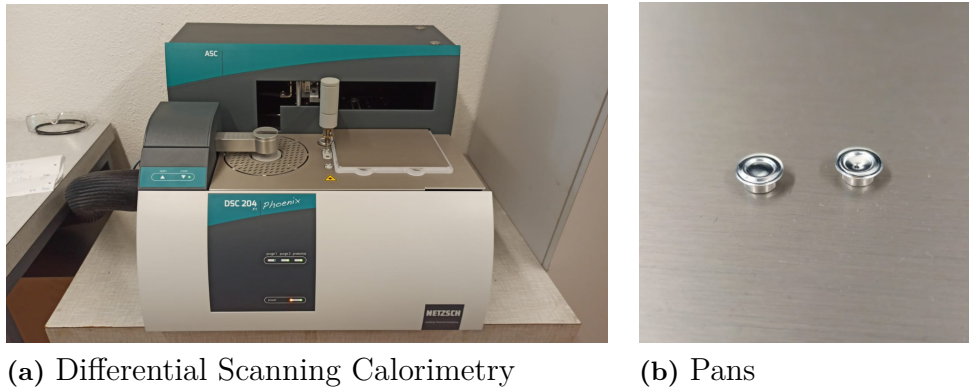


**Figure 3.1:** Standard and Modulated analysis equipment

$$\frac{d\alpha}{dt} = \frac{A \exp\left(-\frac{E}{RT}\right)}{1 + \exp[C(\alpha - (\alpha_C + \alpha_T T))]} \alpha^m (1 - \alpha)^n \quad (3.1)$$

In the formula  $d\alpha/dt$  is the reaction rate,  $\alpha$  the degree of cure,  $T$  the temperature,  $n$  the  $n$ -th order of reaction,  $m$  the autocatalytic order of reaction,  $A$  the pre-exponential Arrhenius factor,  $E$  the activation energy,  $C$  the coefficient controlling the breadth of the transition,  $\alpha_C$  the coefficient governing the chemical-controlled part of the reaction, and  $\alpha_T$  the coefficient governing the diffusion-controlled part of the reaction.

Furthermore, Temperature Modulated (TM) DSC analysis were carried out to evaluate the glass transition region of samples partially cured up to a certain level of degree of cure. The glass transition region represents a phase transformation that leads to a change in the heat capacity of the polymer and it is important to underline that this is a region, not a point. However, for engineering needs the  $T_g$  is commonly calculated as the middle value of the whole region, and it is obtained exploiting the tangent lines which can be drawn before and after the transition region. More than five tests were run and a DiBenedetto curve [32, 33] was modelled to fit the data obtained using the following law:

$$T_g = T_{g_0} + \frac{(T_{g_\infty} - T_{g_0})\lambda\alpha}{1 - (1 - \lambda)\alpha} \quad (3.2)$$

where  $T_g$  is the glass transition temperature,  $T_{g_0}$  the glass transition temperature for the uncured resin,  $T_{g_\infty}$  the glass transition temperature for the fully cured ma-

terial,  $\alpha$  the degree of cure, and  $\lambda$  a fitting parameter controlling the convexity of the non-linear regression.

Every test consisted in a dynamic ramp at 1°C/min up to a certain temperature (e.g. 120°C, 130°C, 140°C, etc), a quick cool down phase at 20°C/min, and a further dynamic ramp at 10°C/min to evaluate the Tg. The result of the fitting of the DiBenedetto curve was then validated by evaluating the Tg of samples of material partially cured at 100°C for different amounts of time (40, 70, 80, and 110 minutes). For each case, two samples were tested, one partially cured in the oven and one partially cured directly in the DSC. In both cases, the isothermal phase was followed by a quick ramp at 20°C/min in the DSC to evaluate the glass transition temperature.

### 3.3 Manufacturing process

The aim of the manufacturing was to produce specimens to be tested for delamination through peel-off tests. The specimens produced were made using dimensions of 13.5 x 290 mm<sup>2</sup> and a total thickness of about 0.4 mm. They were characterised by two layers with a specific partial cure level placed on top of each other. In Table 3.1 it is possible to see combinations of partial cure levels studied in this project. A minimum of three samples was created and tested for every combination. However, the configurations containing layers partially cured up to 20% and 80% were investigated testing at least five specimens, as those levels were thought to require a more thorough analysis with respect to the configurations involving uncured (0%) or fully cured (100%) layers.

		Top Layer			
		DoC %	0	20	80
Bottom Layer	0	0/0	0/20	0/80	0/100
	20		20/20	20/80	20/100
	80			80/80	80/100
	100				100/100

**Table 3.1:** Configurations chosen for the development of the project

The first stage of the manufacturing consisted in partially cure in the oven strips of prepreg. The partial cure was obtained by following cure cycles at 100°C for different periods of time based on the level of partial cure needed. The 20% of degree of

cure was reached heating the strips for 40 minutes, the 80% for 110 minutes, while the full cure of the 100% strips was achieved following the cure cycle presented in the data sheet of the resin system: 1 hour at 120°C and 2 hours at 140°C. The oven used at this stage was a Memmert ©, shown in Figure 3.3.

DoC	$T_{cure}$	$\delta t_{isothermal}$
20%	100°C	40 min
80%	100°C	110 min
100%	120°C + 140°C	1 h + 2 h

**Table 3.2:** Thermal profiles for different degrees of cure

Once the strips were partially cured, the two-layer-laminate could be assembled. A first layer of two strips with the same level of degree of cure was positioned on a peel-ply layer. Then, a crack initiator PTFE film was placed on top of it in order to create an artificial crack of 130 mm as shown in Figure 3.2. Lastly, the second layer of strips was laid upon the previous one. Only for the 20/20, 20/80, and 80/80 configurations four strips were placed next of each other in both layers, so to be able to generate more specimens to test later. Indeed, in these three cases five specimens were tested.

The following stage consisted in finalising the cure of the two-layer-laminate created. As already done for the 100% strips, the cure cycle followed was 1 hour at 120°C and 2 hours at 140°C. However, this time the first hour at 120°C took place in the hot press, where it was possible to apply pressure to the laminate. The pressures initially chosen for the experiments were respectively 1 and 2 bar. The machine used in this stage was a Carver © and is shown in Figure 3.3. The pressure was controlled using a pressure gauge that displayed the oil pressure of the machine. Through a calibration data sheet, it was possible to relate the oil pressure that could be set on the machine to the real pressure applied on the specimen. Finally, the cure was finalised with 2 hours at 140°C in the oven previously used.

Once the laminate had finalised its cure, it was left in the oven to cool down for about three hours so not to generate excessive residual stresses with a sudden change in temperatures. When the temperature of the laminate had reached approximately 50°C, it was taken out and cut so to form specimens of dimension 13.5 x 290 mm<sup>2</sup>. These dimensions were chosen so to be in line with the work and project previously



carried out [10] on the the retention of interfacial properties of AM components.

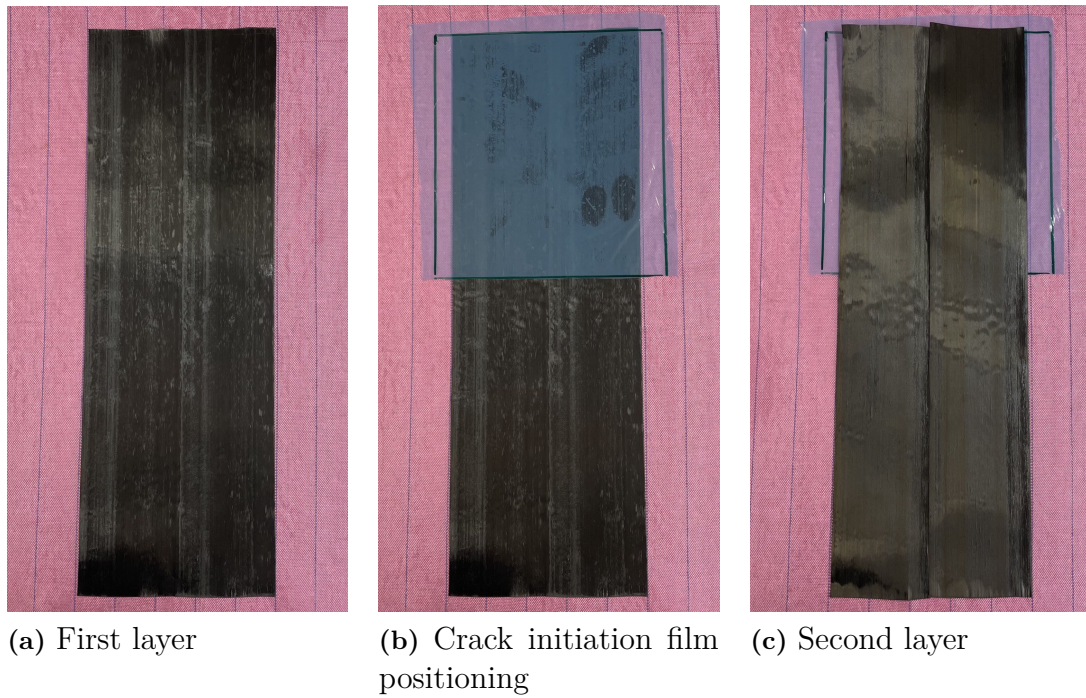


**Figure 3.2:** Manufacturing of the laminate

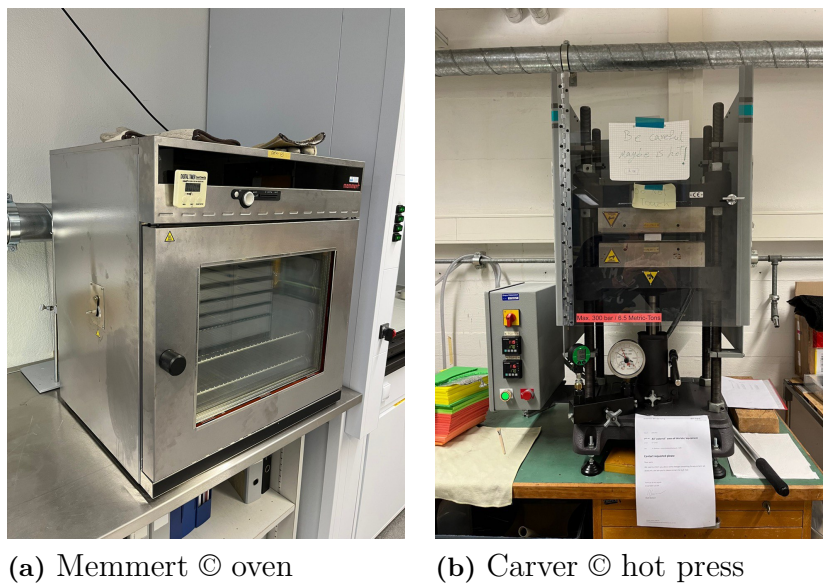


**Figure 3.3:** Equipment used during the manufacturing process



**Figure 3.4:** Specimens obtained from the laminate manufactured

### 3.4 Experimental set up

The Peel-off tests were performed through the use of a Zwick Z010 machine. The set-up of the machine is shown in Figure 3.5.



**Figure 3.5:** Zwick Z010 machine set-up for the peel-off tests

The tests were performed following the ISO 11339:2010 standard, with a load cell of 20 N and a speed rate of 50 mm/min as already done in previous work [10]. The selected speed rate allowed quick tests of about 10 minutes per test while keeping the fibers intact during the peeling. The machine recorded the load to peel-off the two layers against the extension during each test, and the adhesive fracture toughness  $G_A$  was then calculated for each configuration through the use of the following formula:

$$G_A = 2F/w(1 - \cos\theta) \quad (3.3)$$

where  $F$  is the force applied,  $w$  is the width, and  $\theta$  is the peel angle. During these experiments it was considered an ideal case where  $\theta$  was equal to  $90^\circ$ .

## 3.5 Finite Element model

In this section, a mechanical and a coupled thermo-mechanical FE models built on the FE Analysis software MSC Marc Mentat 2022.1 © are presented. The models, the mesh, and the initial and boundary conditions were entirely implemented on Marc ©.

### 3.5.1 Cure kinetics validation

This simulation took into account the case of 0/0 degree of cure configuration, and it aimed at describing the development of the cure in the prepreg used for this project, while checking for thermal gradients through the thickness. For this model, a 3D coupled thermo-mechanical analysis was required. The part modeled is shown in Figure 3.6 and had a dimension of 100 x 290 mm<sup>2</sup> with a total thickness of 0.4 mm. The mesh considered for it consisted in dividing the thickness in ten elements, shown in Figure 3.7, to obtain a finer development of the thermal gradient through it.

Some assumptions were considered to simplify the model. First of all, the pressure applied on the laminate in the hot press was neglected, narrowing the focus of the simulation on the validation of the cure cycle used. Then, the initial conditions taken into account on the part were an initial degree of cure equal to 0.1% to be in line with the model and a uniform initial temperature of 30°C. Finally, the only boundary condition applied to the part is the temperature profile. Both initial and

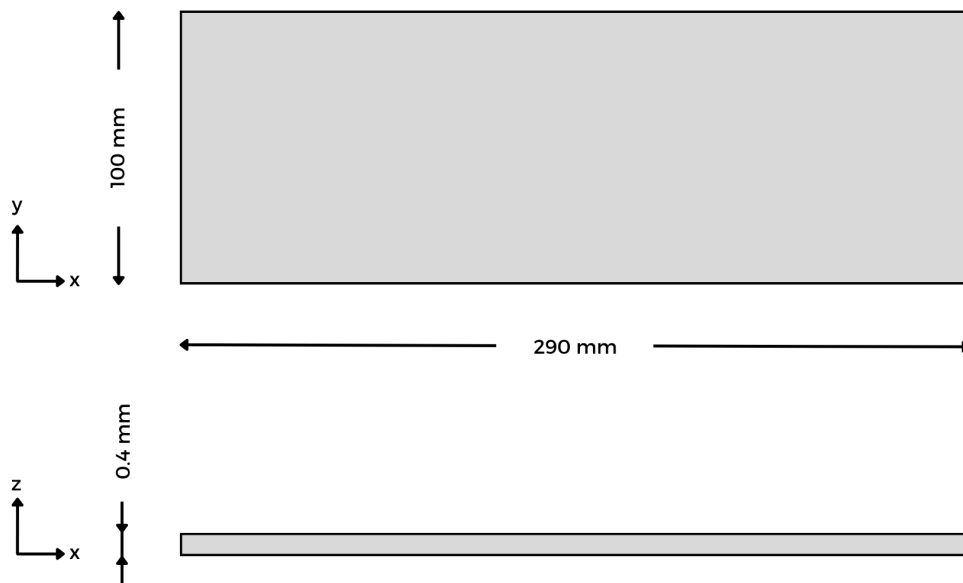


**Figure 3.6:** Schematic model of the dimensions of the component

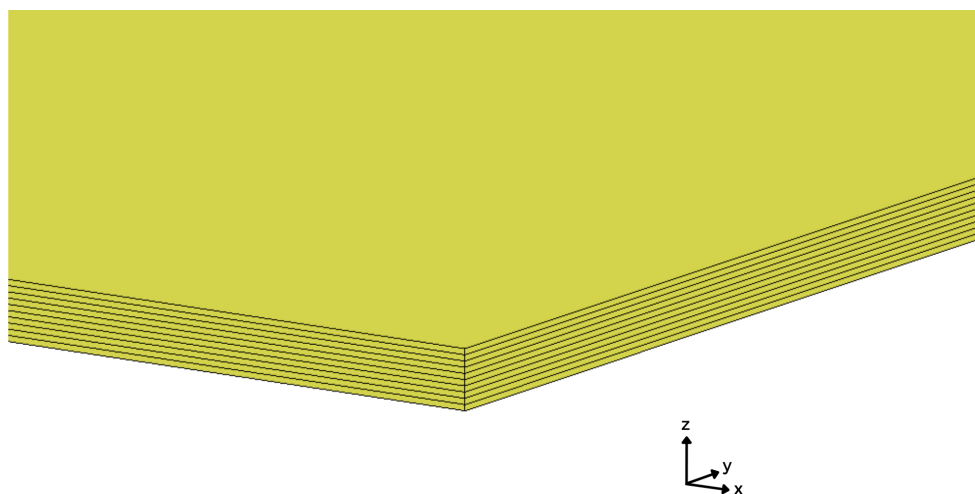


**Figure 3.7:** Mesh of the 0/0 configuration, focus on the thickness of the laminate

boundary conditions were applied to the eight nodes constituting the vertexes of the laminate. Moreover, all the proprieties of the material obtained from [21] are listed in Table 3.3.

<b>Thermal conductivity properties</b>	
$K_1$ [W/m/K]	3.22
$K_2$ [W/m/K]	0.4457
$K_3$ [W/m/K]	0.4457
<b>Specific heat</b>	
$c_p$ [J/kg/K]	942
<b>Mass density</b>	
$\rho_p$ [kg/m <sup>3</sup> ]	1520

**Table 3.3:** Properties of the material

The thermal profile applied on the laminate was implemented through the creation of Tables on the FEA software. The simulation started at room temperature (30°C) and reached an isothermal level of 120°C with a heating rate of 7.5°C/min. The latter was chosen based on the heating rate determined during the manufacturing process in the hot press. The temperature was then maintained constant for 1 hour to fully cure the part. The temperature profile applied can be seen in Figure 3.8, where all the temperatures on the y axis are expressed in degree Kelvin, while on the x axis the time in seconds is displayed.

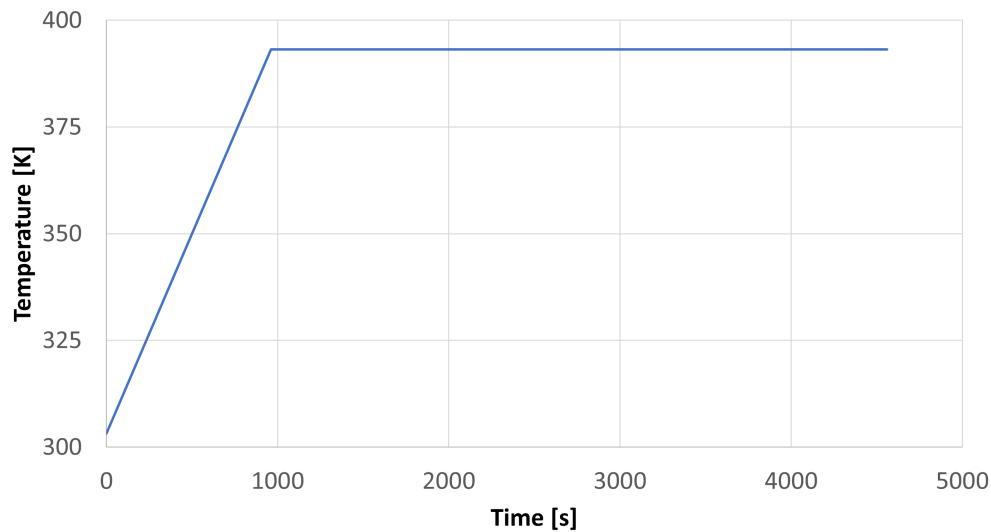


**Figure 3.8:** Temperature profile applied to cure the 0/0 configuration

### 3.5.2 Peel-off tests

This FE model aimed at validating the adhesive delamination tests performed on the specimens. A 3D structural analysis was performed on Marc © to simulate the behaviour of the cohesive bonds of the composite layers. The part generated on the FE software and showed in Figure 3.9 was formed by two layers of composite material and an cohesive interface between them. The two 3D shell laminates had both dimension  $290 \times 13.5 \times 0.2 \text{ mm}^3$  and 232 elements along the length on the x axis, while the 3D cohesive interface had a length of 160 mm to simulate the 130 mm crack of the specimen.

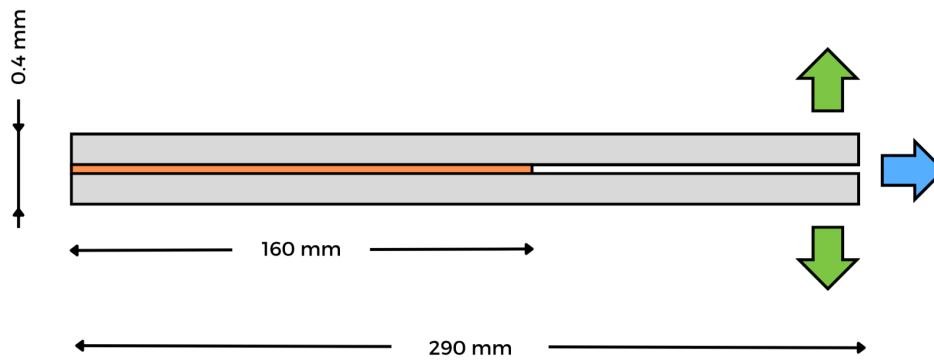


**Figure 3.9:** Schematic model of the part designed on Marc ©

To simplify the experiment conditions, the force needed to peel-off the two layers was applied in the thickness direction only on four symmetric nodes, two in the upper layer and two in the lower one. A focus on the boundary conditions applied on the upper layer of the model can be seen in Figure 3.10. The four nodes chosen represented the portion of material in contact with the machine set-up and directly subjected to the load of the machine. On the same nodes a fixed displacement on the x direction was also considered, so to simulate the real behaviour of the specimen: as the two layers are pulled apart, the remaining material shifts forward. Lastly, a contact body analysis allowed the user to understand how the bodies, which in this specific case were the upper and lower laminates, would deform under the effect of the boundary conditions applied. All the structural properties of the laminate are evaluated through Equations 3.4 - 3.9 and listed in Table 3.4 (a), the parameters used for such calculations can be found in [21]. The mechanical properties of the cohesive interface can be found in Table 3.4 (b), the cohesive energy  $E$  is represented as a constant but will be used as a parameter in the simulations to validate the results of the delamination tests.

$$E_1 = \nu_f E_{1f} + (1 - \nu_f) E_r \quad (3.4)$$

$$E_2 = E_3 = \frac{E_r}{1 - \sqrt{\nu_f} \left(1 - \frac{E_r}{E_{2f}}\right)} \quad (3.5)$$

$$G_{12} = G_{31} = \frac{G_r}{1 - \sqrt{\nu_f} \left(1 - \frac{G_r}{G_{12f}}\right)} \quad (3.6)$$

$$G_{23} = \frac{G_r}{1 - \sqrt{\nu_f} \left(1 - \frac{G_r}{G_{23f}}\right)} \quad (3.7)$$

$$\nu_{12} = \nu_{31} = \nu_f \nu_{12f} + (1 - \nu_f) \nu_r \quad (3.8)$$

$$\nu_{23} = \frac{E_2}{2G_{23}} - 1 \quad (3.9)$$

<b>Young's Moduli</b>	
$E_1$ [N/m <sup>2</sup> ]	1.46e11
$E_2$ [N/m <sup>2</sup> ]	1.14e10
$E_3$ [N/m <sup>2</sup> ]	1.14e10
<b>Poisson's Ratios</b>	
$\nu_{12}$ [-]	0.245
$\nu_{23}$ [-]	0.425
$\nu_{31}$ [-]	0.245
<b>Shear Moduli</b>	
$G_{12}$ [N/m <sup>2</sup> ]	6.3e9
$G_{23}$ [N/m <sup>2</sup> ]	4e9
$G_{31}$ [N/m <sup>2</sup> ]	6.3e9

(a) Laminate

<b>Cohesive Energy</b>	
E [N/m]	200
<b>Critical Opening Displacement</b>	
COD [m]	3e-4
<b>Shear/Normal Coefficients</b>	
Maximum stress [-]	1
Cohesive energy [-]	1

(b) Cohesive interface

**Table 3.4:** Properties of the materials

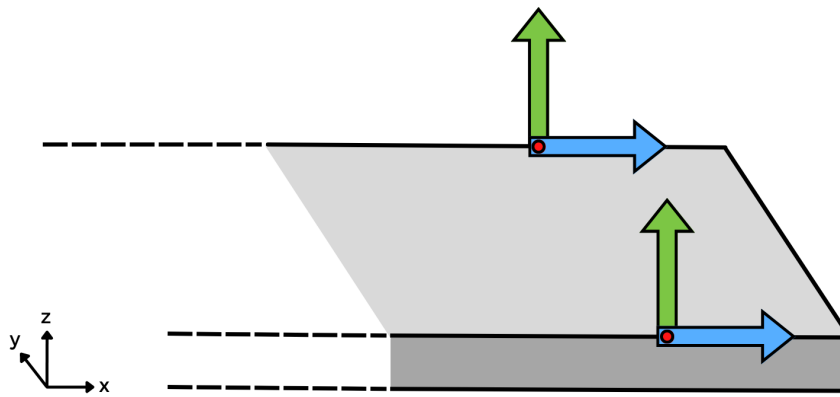


**Figure 3.10:** Boundary conditions applied on two nodes of the upper layer of the model



---

# 4

## Results and Discussion

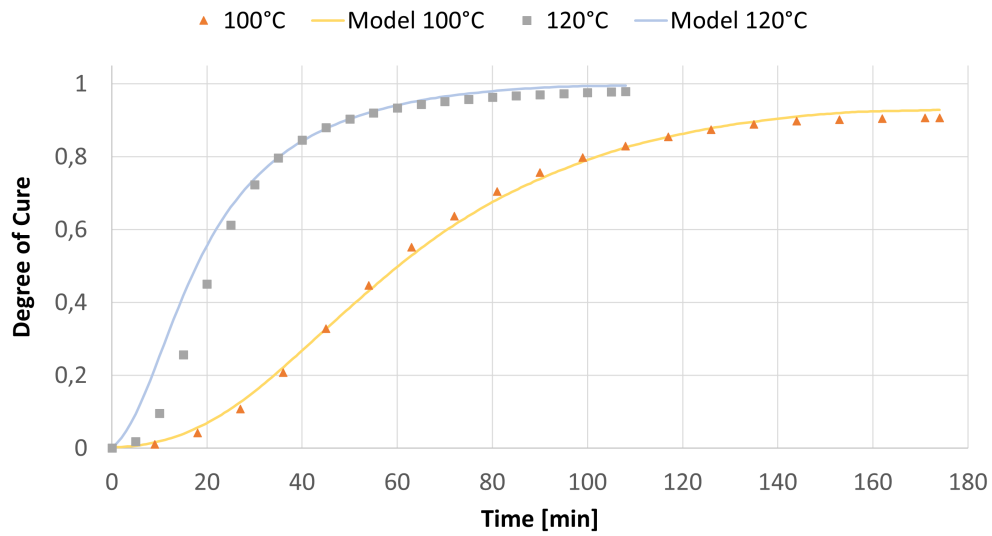
In this chapter, the results of the characterisation of the resin system in the material used, the peel-off tests performed to address the mechanical properties of the specimens manufactured, and the outcomes of the FE models are presented and analysed.

### 4.1 Cure kinetics

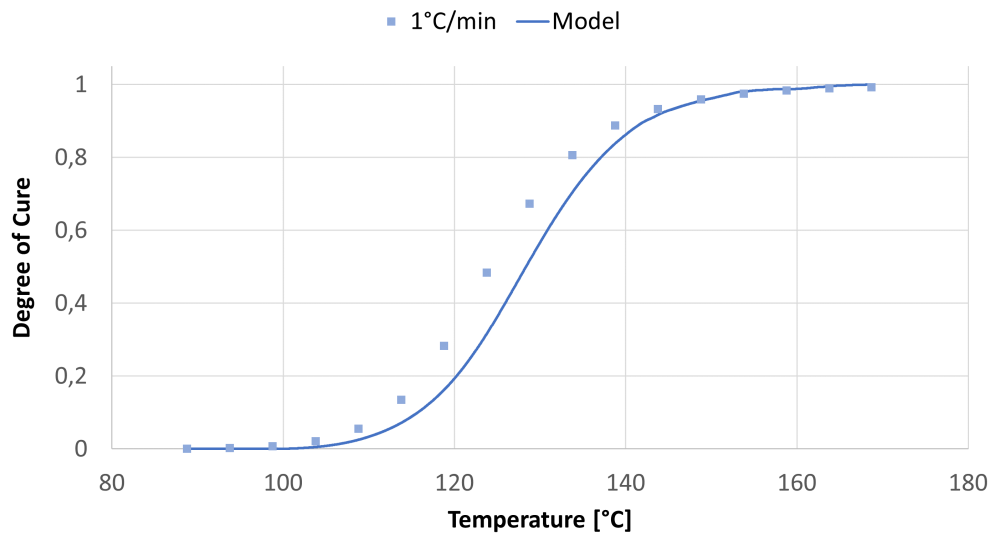
The post-processing of the experimental data obtained by running the DSC testing campaign described in Section 3.2 resulted in the characterisation of the cure kinetics through a phenomenological model. All the parameters of Equation 3.1 were tuned to get the best fitting achievable for the isothermal and dynamic curves, as shown in Figure 4.1 . Moreover, the fitting parameters are reported in Table 4.1. The accuracy of the fitting is equal to 98.88% and was calculated through the R-square coefficient, defined as the square of the Pearson product-moment correlation coefficient, which ranges between zero and one, where one is the perfect fitting.

Parameter	Value
n [-]	1.569
m [-]	0.72
A [s <sup>-1</sup> ]	1.08e+06
C [-]	174.449
E [J/mol]	64697.639
$\alpha_C$ [-]	-0.97
$\alpha_T$ [K <sup>-1</sup> ]	0.005
H <sub>tot</sub> [J/kg]	352000

**Table 4.1:** Cure kinetics fitting parameters



(a) Fitting of isothermal runs



(b) Fitting of dynamic runs

**Figure 4.1:** Characterisation of the cure kinetics

The TM-DSC tests run to assess the inflection point of the glass transition region of partially cured samples led to the modelling of the DiBenedetto curve. The data obtained exploiting Equation 3.2 were fitted as shown in Figure 4.2, where they are represented as white squares. The DiBenedetto parameters are listed in Table 4.2. As explained in Section 3.2, the fitting of the DiBenedetto curve was validated by running TM-DSC analysis on samples of prepreg partially cured at 100°C for different amounts of time either in the oven or through the DSC. The data obtained from the modulated tests are shown in Figure 4.2 as blue triangles and are in line with the fitting of the DiBenedetto curve.

Parameter	Value
$T_{g_0}$ [°C]	7.784
$T_{g_\infty}$ [°C]	118.728
$\lambda$ [-]	0.238

**Table 4.2:** DiBenedetto parameters

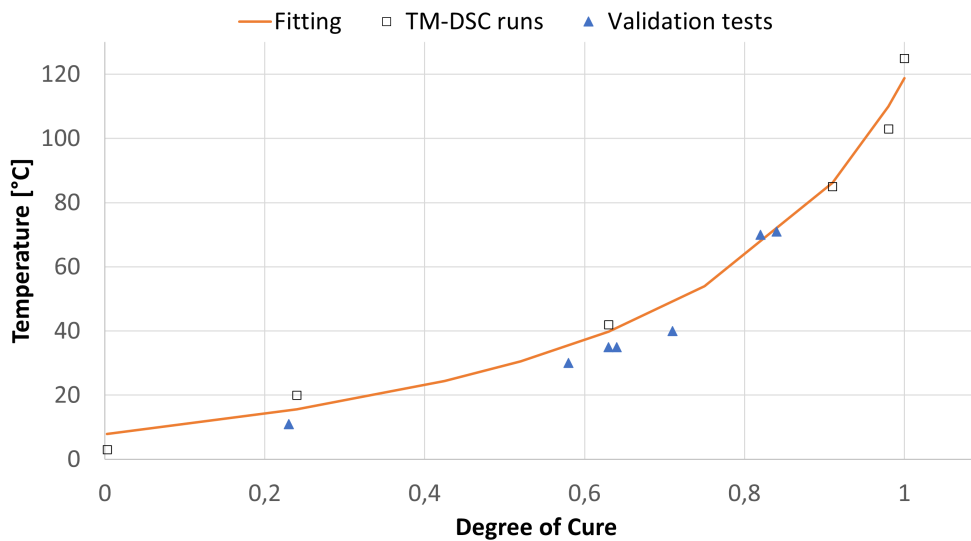


**Figure 4.2:** DiBenedetto curve

## 4.2 Peel-off tests

In Chapter 3 the set up for the peel-off tests is presented. This section presents and discusses the results obtained from the debonding experiments at different pressures, starting from 1 bar, to address the modification of the interfacial properties. The tensile Zwick machine used recorded and plotted the load to peel-off two layers against the extension. The adhesive fracture toughness  $G_A$  was then calculated through Equation 3.3 and plotted against the extension. For each configuration,  $G_A$  was determined as the average of either three or five tests after identifying a steady state window of the curve plotted. It was necessary to do so, since the data were strongly affected by bridging, causing the fracture toughness to increase its value while the crack opened. For repeatability, the window was chosen to be 100 mm wide and to start right after the crack propagation was reached. For instance, the window chosen for the configuration 0/20 at 1 bar is the interval between 220 and 320 mm as visible in Figure 4.3.

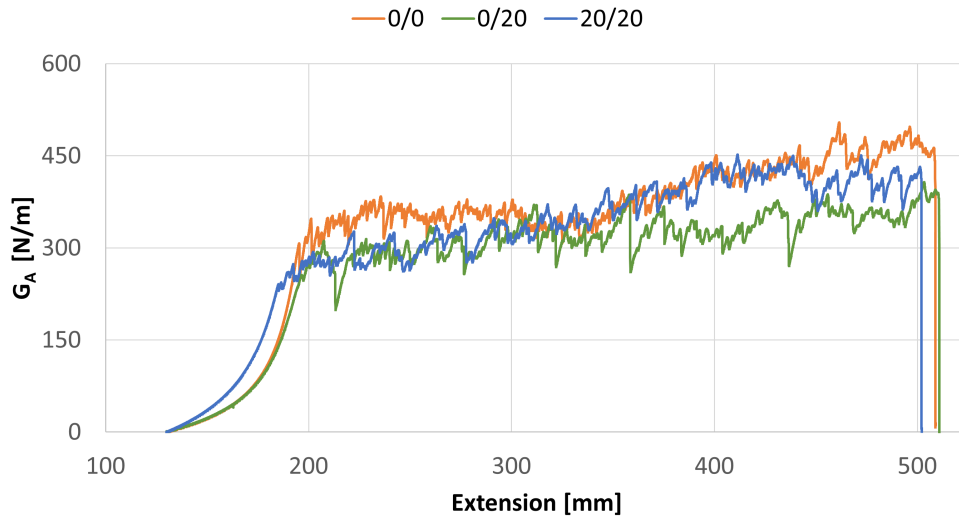


**Figure 4.3:** Configurations with two layers below gelation (1 bar consolidation pressure)

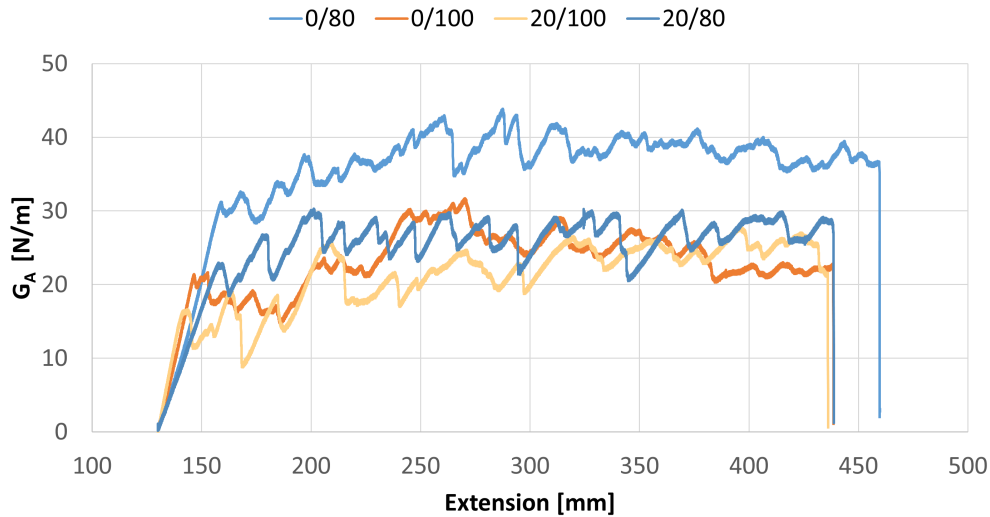


**Figure 4.4:** Configurations with one layer above gelation (1 bar consolidation pressure)

Figure 4.3 highlights that when both of the two layers are below the gelation point, the mechanical properties are mostly retained. A small drop in the value of  $G_A$  of about 15% is visible in configurations 0/20 and 20/20. The layout 0/0 is identified by the highest value of  $G_A$ ; however, it is not of interest as the aim of this research is to determine the best level of partial cure of the layers to avoid the cure of the whole part all at once, with the risk of generating residual stresses and defects in the component. Figure 4.4 focuses on the configurations which are characterised by one layer above the gelation point. For these, it is clear that the mechanical

properties are not retained, causing a drop of  $G_A$  of about 90% with respect to all the configurations in which no layer was above the gelation point. Finally, it is important to underline the issues encountered during the manufacturing of the configurations characterised by both layers above the gelation point (80/80, 80/100, 100/100). For these configuration, no tests were performed since the high level of partial cure did not allow any bonding between the two layers, as no more cross-linking was possible. Hence, the adhesive fracture toughness of these layouts is 0 N/m. Table 4.3 presents the average values of  $G_A$  of the configurations tested in case of consolidation pressure equal to 1 bar with the related standard deviations.

		Top Layer			
		DoC %	0	20	80
Bottom Layer	0	353 ± 35	296 ± 23	38 ± 2	30 ± 6
	20		293 ± 27	30 ± 5	20 ± 5
	80			0	0
	100				0

**Table 4.3:** Average  $G_A$  and relative standard deviation for configurations at 1 bar of consolidation pressure

		Top Layer			
		DoC %	0	20	80
Bottom Layer	0	351 ± 37	322 ± 72	43 ± 8	29 ± 4
	20		244 ± 41	33 ± 2	24 ± 1
	80			0	0
	100				0

**Table 4.4:** Average  $G_A$  and relative standard deviation for configurations at 2 bar of consolidation pressure

The second set of experiments was performed on the configurations manufactured under a 2 bar pressure condition. The results obtained from the delamination tests are recorded in Table 4.4 and show similar trends to the ones of the previously described layouts whose cure was carried out at 1 bar. This is shown in Figure 4.5, where a bar chart compares the average values of  $G_A$  for the configurations at 1 and 2 bar of consolidation pressure. The lack of visible changes in the behaviour of the

material could be explained by two different scenarios. In the first case, it can be understood that 1 bar is the optimum consolidation pressure hence, further increase of pressure does not lead to improvements in the cohesive bonding of the layers, and a better performance could be obtained at lower consolidation pressures. In the second case, the two pressures chosen are too similar to see a change in the behaviour of the mechanical properties and thus, higher pressures must be considered to obtain visible improvements. These considerations led to the decision of analysing the 0/20 configuration when subjected to other two consolidation pressures: 0.5 bar and 10 bar.

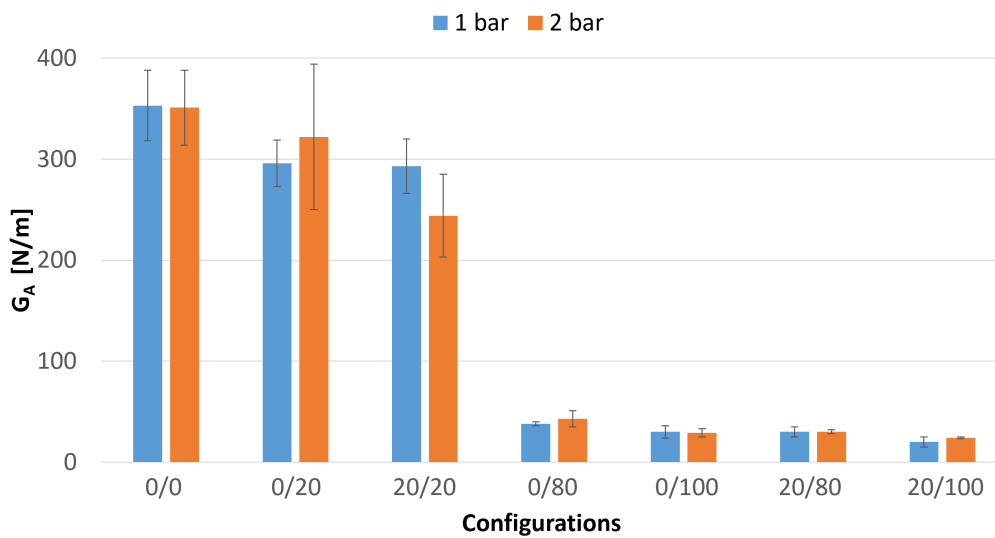
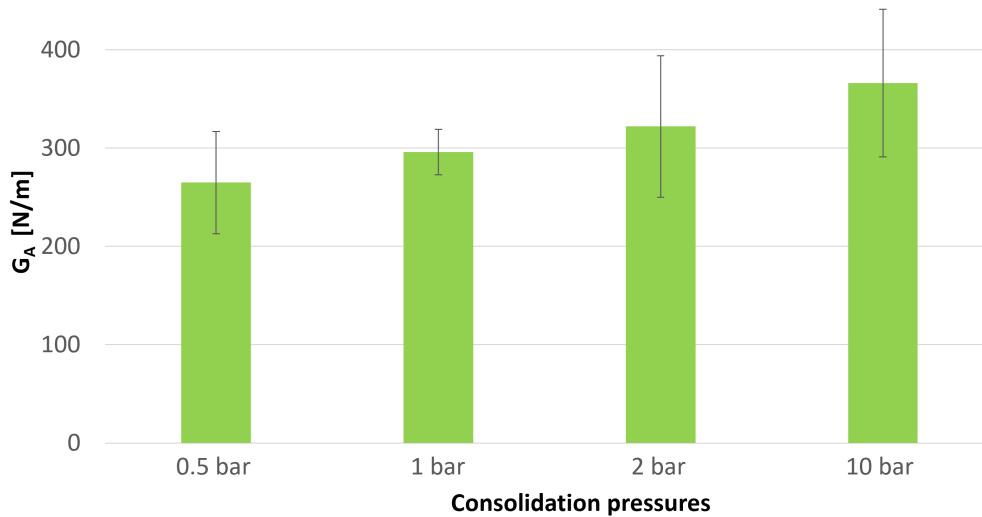


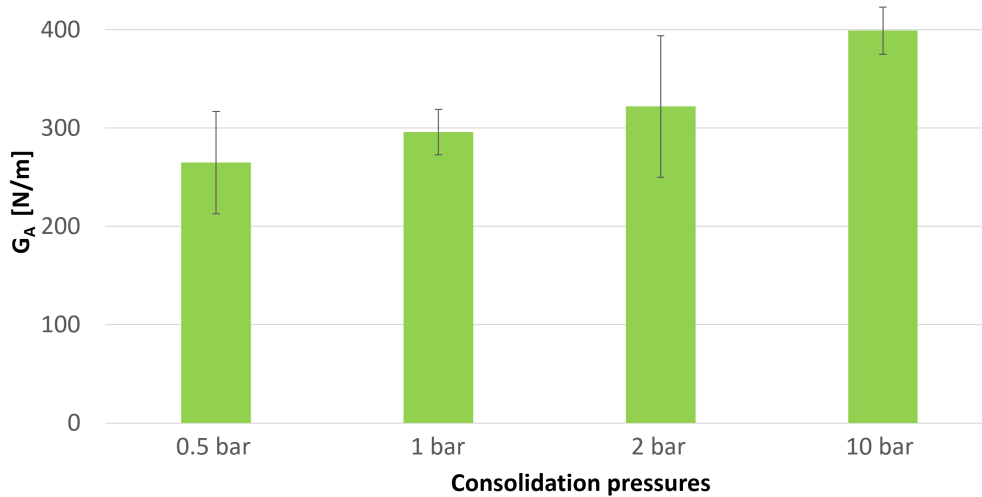
**Figure 4.5:** Comparison between average  $G_A$  for configurations at 1 bar and 2 bar of consolidation pressure

The results of the peel-off tests performed on the 0/20 configurations consolidated at different pressures are reported in the bar chart in Figure 4.6. It can be seen that the standard deviation error bars overlap in case of 0.5, 1, and 2 bar consolidation pressure. Thus, those cases do not show a statistically significant difference in fracture toughness, and the interfacial properties of the material are expected to behave similarly. The  $G_A$  of the specimens tested for 10 bar of consolidation pressure are presented in Figure 4.7. Out of the five specimens tested for delamination, one registered a fracture toughness lower than expected and was addressed as an outlier. It was not possible to establish whether this test could be discarded due to experimental errors and thus, it was kept among the results. However, it is important to highlight that its presence affects greatly the average fracture toughness and its standard deviation. In Figure 4.6 two scenarios are shown, one where the outlier is taken into consideration and one where it is neglected. In case the outlier

curve was found out to be the result of experimental or manufacturing errors, it could be stated that an increase of consolidation pressure up to 10 bar can have a beneficial effect in terms of interfacial properties. To fully address this matter, further experiments should be carried out for different significant configurations (two layers below gelation point) consolidated at 10 bar.



(a) Outlier is considered



(b) Outlier is neglected

**Figure 4.6:** Comparison between average  $G_A$  for the 0/20 configuration at different consolidation pressures

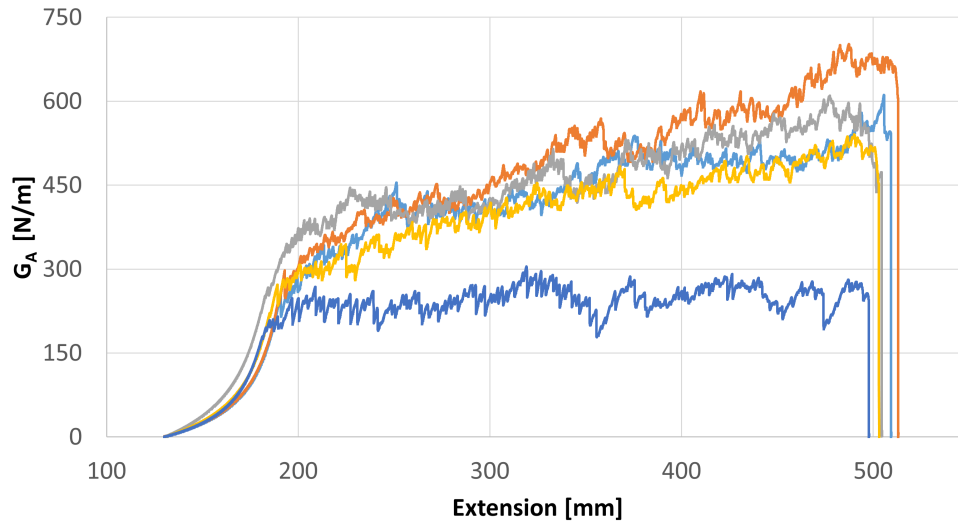


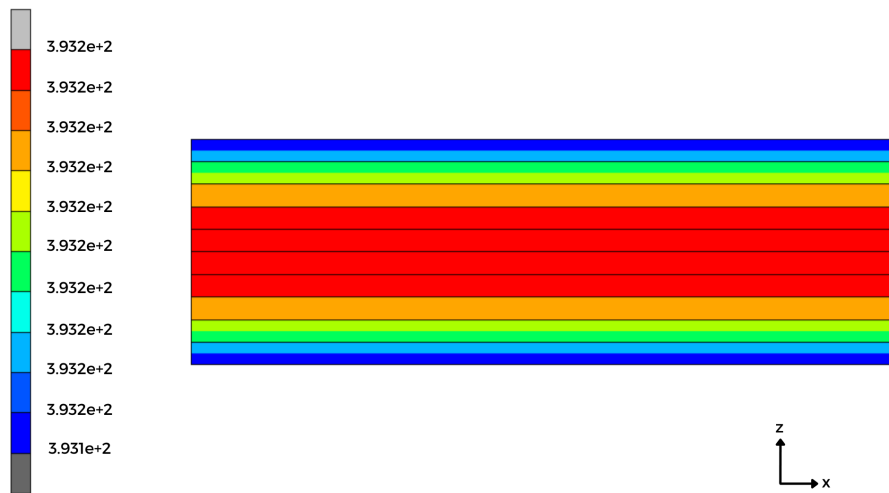
**Figure 4.7:** 0/20 configuration at 10 bar of consolidation pressure

## 4.3 Finite Element model

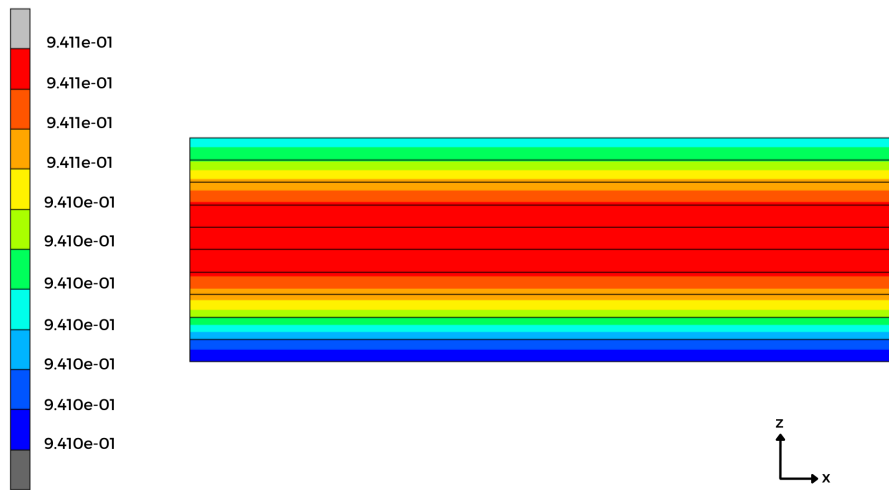
### 4.3.1 Cure kinetics validation

The FE model is used to verify that no gradients of temperatures are present along the thickness direction and that the degree of cure is uniform in that direction, with the aim of being able to fully trust the phenomenological model built without having to run simulations. Figure 4.8 shows that across the thickness both the temperature and the degree of cure are uniform. Furthermore, in Figure 4.9 the model of the cure kinetics obtained through the characterisation campaign described in Section 3.2 is compared with the evolution of the degree of cure with respect to time obtained from the FE model. The curves overlap almost completely, and the difference between the two is due to a more refined time step in the FE simulation. Moreover, for an exhaustive understanding of the kinetics model, experimental uncertainties as the human factor were taken into account. Indeed, while curing the laminates, the speed at which the manufacturer introduces and removes the material in and out the hot press could vary the total time of finalisation of the cure of about  $\pm 1$  minute. By looking at the cure kinetics and the FE model, it was proven that this range is responsible for a shift in degree of cure of circa  $\pm 0.2\%$ .





(a) Temperature gradient across the thickness; the temperatures in the colourmap are in Kelvin



(b) Degree of cure across the thickness

**Figure 4.8:** Validation of the cure kinetics

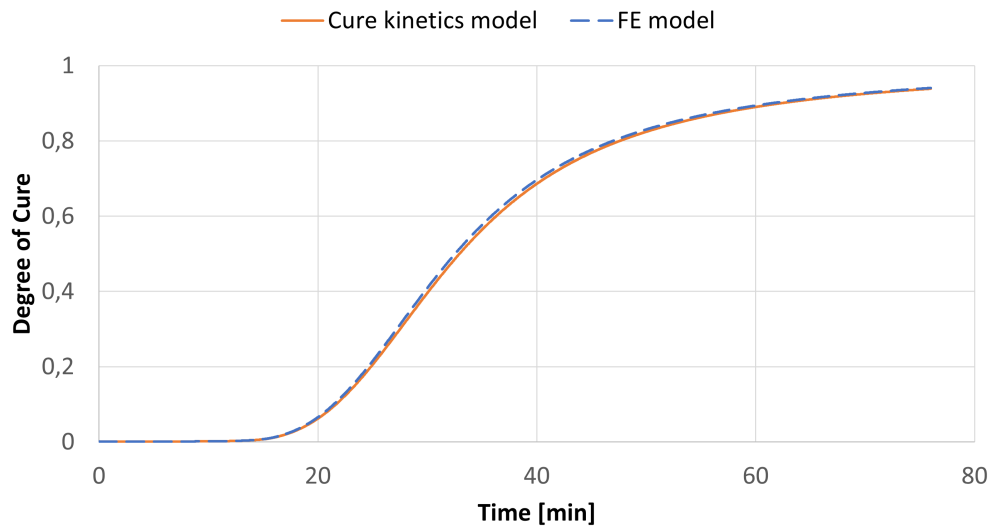


**Figure 4.9:** Comparison between the model of the cure kinetics and the FE model

### 4.3.2 Peel-off tests

This FE model was used as an assessment of the analysis of the peel-off tests performed. The simulation was run setting the parameter of cohesive energy showed in Table 3.4 (b) equal to values of fracture toughness obtained from the delamination tests. The values chosen were 306.09 N/m, obtained testing one specimen of the 0/20 configuration at 1 bar, and 21.43 N/m, obtained from one specimen of the configuration 20/100 at 1 bar.

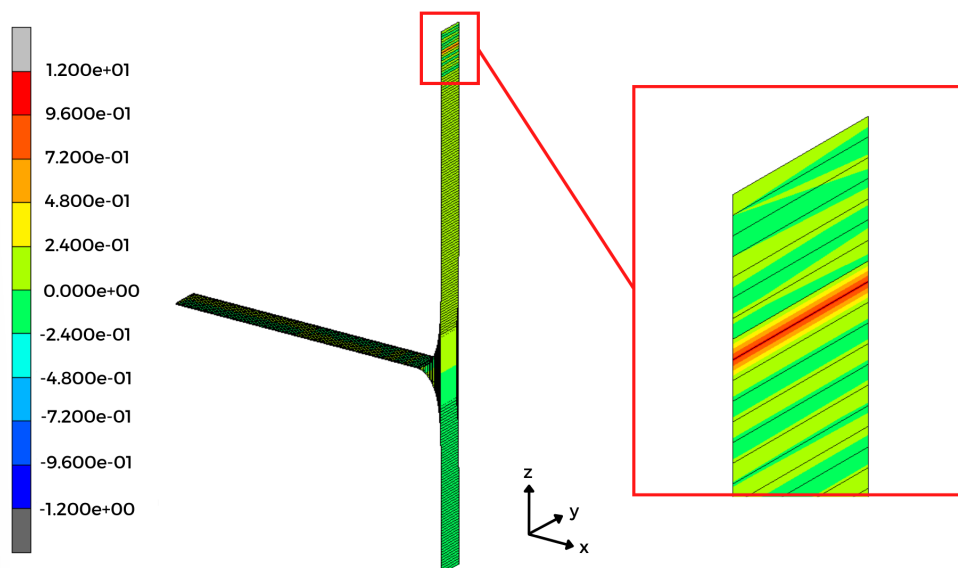


**Figure 4.10:** FE simulation for  $G_A$  equal to 306.09 N/m and focus on the upper nodes simulating the contact with the peel-off machine; the reaction force in the colourmap is in N

For the first scenario, the reaction force in the z direction, with a focus on the upper nodes region, is shown in Figure 4.10. Moreover, the values of the reaction forces applied to the upper and lower nodes are plotted against the extension up to 250 mm in Figure 4.11. It can be seen that each of the two layers is undergoing a total reaction force of about 1 N. This outcome is in line with the results obtained during the delamination tests, where a total reaction force of 2 N was registered. The same graph is also reported in Figure 4.12 for the second scenario where the fracture toughness introduced in the model is 21.43 N/m. Finally, Table 4.5 summarises the values of reaction force in the z direction achieved through delamination tests and compares them with the ones obtained from the FE model, assessing that the simulation is able to represent the real behaviours of the delamination tests and that the analysis carried out, including the approximate relation between fracture toughness and peel force, is valid.

$G_A$ [N/m]	$F_z$ Peel-off test [N]	$F_z$ FE model [N]
306.09	2.10	2.05
21.43	0.15	0.15

**Table 4.5:**  $F_z$ : comparison between delamination tests and FE simulations

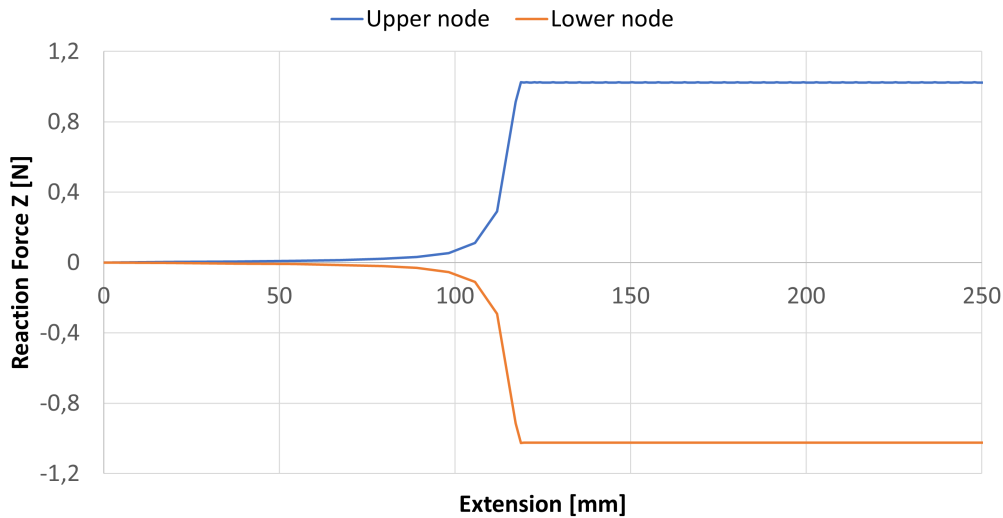


**Figure 4.11:** Reaction Force Z on the nodes of the FE model for  $G_A$  equal to 306.09 N/m

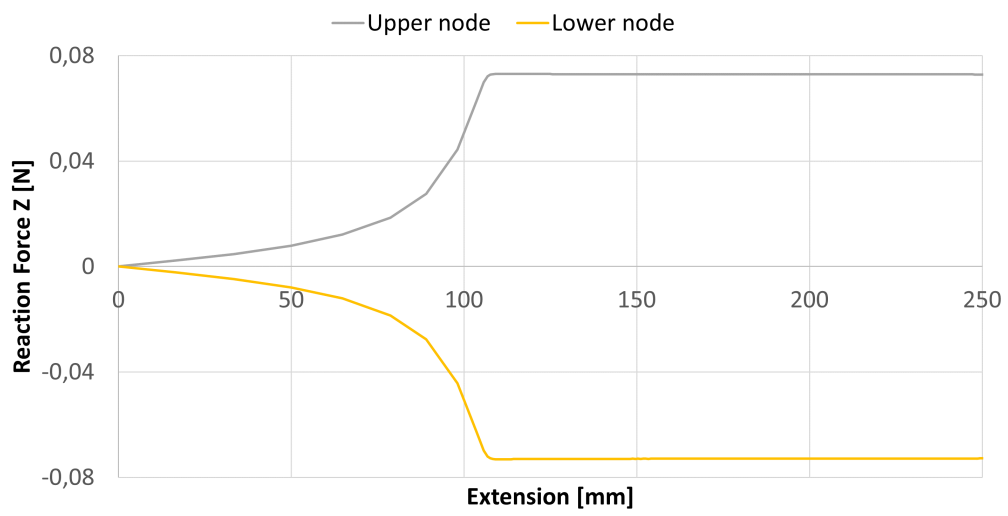


**Figure 4.12:** Reaction Force Z on the nodes of the FE model for  $G_A$  equal to 21.43 N/m

---

# 5

## Conclusions and Future Work

This chapter summarises the results obtained and addresses future developments of the project.

### 5.1 Conclusions

The characterisation of the cure kinetics of the resin system present in the material was performed through standard and TM-DSC analysis and was identified by an accuracy of 98.88%. This characterisation led to the choice of the cure cycle (temperature and time) followed to partially cure the prepreg strips. The manufacturing of samples with different degree of cure and consolidation pressures was carried out and delamination tests (ISO 11339:2010 standard) were performed to investigate the effect of pressure on partially cured parts. Finally, a thermo-mechanical and a structural FE model were built in order to simulate the consolidation process and the delamination experiments.

The peel-off tests performed allowed to address the effect of both partial cure and pressure on the bonding between two layers of material. The fracture toughness of the specimens was mapped against the degree of cure of the configuration analysed and it was proven to be maximum when the layers bonded together did not undergo partial cure (0/0 configuration). The aim of this manuscript was to search for the best level of partial cure to apply in order to achieve good interfacial properties in the bonding, and this was shown to happen when both layers were partially cured below the gelation point of the material (0/20, 20/20 configurations). When consolidated at 1 bar, these configurations registered a drop of 15% in fracture toughness with respect to the uncured configuration. Moreover, comparing the results coming from two 0/20 configurations consolidated at either 1 or 10 bar, there is evidence that an increase of pressure up to 10 bar could have beneficial effects in terms of interfacial properties. Nevertheless, to gain a complete understanding of how much the increase of pressure affects the interfacial properties, further delamination tests

should be carried out on configurations characterised by two layers below gelation and consolidated at 10 bar.

The Finite Element models built validated successfully both the cure process and the analysis of the delamination tests performed. For the consolidation process, it was determined that it is possible to fully trust the phenomenological model of the cure kinetics, without having to run simulations. The structural analysis simulating the peel-off tests employed cohesive elements and contact bodies to reproduce the real behaviours of the experiments and validated the analysis accomplished, even though approximations were introduced in the model, as the linearisation of the relationship between peel force and fracture toughness.

### 5.2 Future work

Further experiments and investigations are needed to complete the study on how pressure and degree of cure affect the bonding between layers of CFRPs. In particular, further assessments should consider:

- Additional experiments on configurations with both layers below gelation and consolidated at 10 bar, to fully understand if the increase of pressure can lead to positive effects on the interfacial properties of the material. This investigation should also be able to determine if the outlier present in the configuration 0/20 at 10 bar described in section 4.2 was due to experimental or manufacturing errors.
- Acquiring images through a Scanning Electron Microscope (SEM) to address the surface state of the samples after the delamination tests and evaluate the effects of partial cure upon the failure mode. This is expected to be cohesive for configurations where both layers are below gelation, while it is likely to be mainly through the interface for those configurations where the two layers did not fully bond.
- Further experiments on mode II and III fracture toughness to expand this study, which is focused on mode I. This is necessary to gain information on how to produce a part which can perform well under all type of fracture modes, resulting in a high quality of the component manufactured.

- Expansion of the experimental dataset to a range of temperatures and pressures for different partial cure state. This could allow the development of a bonding model methodology for thermosetting interfaces.





---

# Bibliography

- [1] A. Katunin, K. Krukiewicz, A. Herega, and G. Catalanotti, “Concept of a conducting composite material for lightning strike protection,” *Advances in Materials Science*, vol. 16, no. 2, p. 32, 2016.
- [2] G. Marsh, “Composites flying high,” *Reinforced plastics*, vol. 58, no. 3, pp. 14–18, 2014.
- [3] G. Struzziero and J. J. E. Teuwen, “A fully coupled thermo-mechanical analysis for the minimisation of spring-in and process time in ultra-thick components for wind turbine blades,” *Composites Part A: Applied Science and Manufacturing*, vol. 139, p. 106105, 2020.
- [4] J. Rybicka, A. Tiwari, P. A. Del Campo, and J. Howarth, “Capturing composites manufacturing waste flows through process mapping,” *Journal of Cleaner Production*, vol. 91, pp. 251–261, 2015.
- [5] G. Struzziero and J. J. E. Teuwen, “Effect of convection coefficient and thickness on optimal cure cycles for the manufacturing of wind turbine components using vartm,” *Composites Part A: Applied Science and Manufacturing*, vol. 123, pp. 25–36, 2019.
- [6] G. Struzziero and A. A. Skordos, “Multi-objective optimisation of the cure of thick components,” *Composites Part A: Applied Science and Manufacturing*, vol. 93, pp. 126–136, 2017.
- [7] A. A. Skordos and J. Kratz, “Layer by layer curing (lbl) feasibility study final report.”
- [8] A. Baldan, “Adhesion phenomena in bonded joints,” *International Journal of Adhesion and Adhesives*, vol. 38, pp. 95–116, 2012.
- [9] M. D. Banea and L. F. da Silva, “Adhesively bonded joints in composite materials: an overview,” *Proceedings of the Institution of Mechanical Engineers, Part L: Journal of Materials: Design and Applications*, vol. 223, no. 1, pp. 1–18, 2009.
- [10] A. Gilbert, “Influence of pre-curing upon printability and interlaminar properties in thick composites manufactured by additive manufacturing,” Master’s

- thesis, Cranfield University, School of Aerospace, Transport and Manufacturing, 2021.
- [11] S. Piles Guillem, “Delamination behaviour of partially cured laminates,” Master’s thesis, 2013.
- [12] Z.-S. Guo, S. Du, and B. Zhang, “Temperature field of thick thermoset composite laminates during cure process,” *Composites science and technology*, vol. 65, no. 3-4, pp. 517–523, 2005.
- [13] Y. Nawab, X. Tardif, N. Boyard, V. Sobotka, P. Casari, and F. Jacquemin, “Determination and modelling of the cure shrinkage of epoxy vinyl ester resin and associated composites by considering thermal gradients,” *Composites Science and Technology*, vol. 73, pp. 81–87, 2012.
- [14] Y. Nawab, S. Shahid, N. Boyard, and F. Jacquemin, “Chemical shrinkage characterization techniques for thermoset resins and associated composites,” *Journal of Materials Science*, vol. 48, no. 16, pp. 5387–5409, 2013.
- [15] V. Pillai, A. Beris, and P. Dhurjati, “Heuristics guided optimization of a batch autoclave curing process,” *Computers & chemical engineering*, vol. 20, no. 3, pp. 275–294, 1996.
- [16] E. Ruiz and F. Trochu, “Numerical analysis of cure temperature and internal stresses in thin and thick rtm parts,” *Composites Part A: Applied Science and Manufacturing*, vol. 36, no. 6, pp. 806–826, 2005.
- [17] S. Yi and H. H. Hilton, “Effects of thermo-mechanical properties of composites on viscosity, temperature and degree of cure in thick thermosetting composite laminates during curing process,” *Journal of Composite Materials*, vol. 32, no. 7, pp. 600–622, 1998.
- [18] S. Laik, “Influence of residual stress upon the mechanical properties of carbon/epoxy composites,” Ph.D. dissertation, Cranfield University, School of Applied Sciences, Advanced Materials, 2011.
- [19] H. McManus, “Stress and damage in polymer matrix composite materials due to material degradation at high temperatures,” in *35th Structures, Structural Dynamics, and Materials Conference*, 1996, p. 1395.
- [20] J. Li, S. C. Joshi, and Y. C. Lam, “Curing optimization for pultruded composite sections,” *Composites Science and Technology*, vol. 62, no. 3, pp. 457–467, 2002.
- [21] T. A. Bogetti and J. W. Gillespie Jr, “Process-induced stress and deformation in thick-section thermoset composite laminates,” *Journal of composite materials*, vol. 26, no. 5, pp. 626–660, 1992.
- [22] S. R. White and H. T. Hahn, “Cure cycle optimization for the reduction of processing-induced residual stresses in composite materials,” *Journal of Com-*

- posite Materials*, vol. 27, no. 14, pp. 1352–1378, 1993.
- [23] E. Ruiz and F. Trochu, “Multi-criteria thermal optimization in liquid composite molding to reduce processing stresses and cycle time,” *Composites Part A: Applied Science and Manufacturing*, vol. 37, no. 6, pp. 913–924, 2006.
- [24] P. Lopez-Cruz, J. Laliberté, and L. Lessard, “Investigation of bolted/bonded composite joint behaviour using design of experiments,” *Composite Structures*, vol. 170, pp. 192–201, 2017.
- [25] F. Gamdani, R. Boukhili, and A. Vadean, “Tensile behavior of hybrid multi-bolted/bonded joints in composite laminates,” *International Journal of Adhesion and Adhesives*, vol. 95, p. 102426, 2019.
- [26] A. Atas, G. Mohamed, and C. Soutis, “Modelling delamination onset and growth in pin loaded composite laminates,” *Composites Science and Technology*, vol. 72, no. 10, pp. 1096–1101, 2012.
- [27] X. Li, Z. Tan, L. Wang, J. Zhang, Z. Xiao, and H. Luo, “Experimental investigations of bolted, adhesively bonded and hybrid bolted/bonded single-lap joints in composite laminates,” *Materials Today Communications*, vol. 24, p. 101244, 2020.
- [28] G. Kelly, “Load transfer in hybrid (bonded/bolted) composite single-lap joints,” *Composite structures*, vol. 69, no. 1, pp. 35–43, 2005.
- [29] G. Scarselli, C. Corcione, F. Nicassio, and A. Maffezzoli, “Adhesive joints with improved mechanical properties for aerospace applications,” *International journal of adhesion and adhesives*, vol. 75, pp. 174–180, 2017.
- [30] G. Kelly, “Quasi-static strength and fatigue life of hybrid (bonded/bolted) composite single-lap joints,” *Composite structures*, vol. 72, no. 1, pp. 119–129, 2006.
- [31] K. C. Shin and J. J. Lee, “Effects of manufacturing parameters on the tensile load bearing capacity of a co-cured single lap joint,” *J. Mater. Process. Technol.*, vol. 138, pp. 89–96, 2003.
- [32] J. P. Pascault and R. J. J. Williams, “Glass transition temperature versus conversion relationships for thermosetting polymers,” *Journal of Polymer Science Part B: Polymer Physics*, vol. 28, no. 1, pp. 85–95, 1990.
- [33] G. Struzziero, B. Remy, and A. A. Skordos, “Measurement of thermal conductivity of epoxy resins during cure,” *Journal of Applied Polymer Science*, vol. 136, no. 5, p. 47015, 2019.